

Is spatial information in ICT data reliable?

Maxime Lenormand,^{1,*} Thomas Louail,^{2,3} Marc Barthelemy,^{4,5} and José J. Ramasco²

¹*Irstea, UMR TETIS, 500 rue François Breton, FR-34093 Montpellier, France*

²*Instituto de Física Interdisciplinar y Sistemas Complejos IFISC (CSIC-UIB), Campus UIB, ES-07122 Palma de Mallorca, Spain*

³*CNRS, UMR 8504 Géographie-Cités, 13 rue du four, FR-75006 Paris, France*

⁴*Institut de Physique Théorique, CEA-CNRS (URA 2306), FR-91191, Gif-sur-Yvette, France*

⁵*CAMS, EHESS-CNRS (UMR 8557), 190-198 avenue de France, FR-75013 Paris, France*

An increasing number of human activities are studied using data produced by individuals' ICT devices. In particular, when ICT data contain spatial information, they represent an invaluable source for analyzing urban dynamics. However, there have been relatively few contributions investigating the robustness of this type of results against fluctuations of data characteristics. Here, we present a stability analysis of higher-level information extracted from mobile phone data passively produced during an entire year by 9 million individuals in Senegal. We focus on two information-retrieval tasks: (a) the identification of land use in the region of Dakar from the temporal rhythms of the communication activity; (b) the identification of home and work locations of anonymized individuals, which enable to construct Origin-Destination (OD) matrices of commuting flows. Our analysis reveal that the uncertainty of results highly depends on the sample size, the scale and the period of the year at which the data were gathered. Nevertheless, the spatial distributions of land use computed for different samples are remarkably robust: on average, we observe more than 75% of shared surface area between the different spatial partitions when considering activity of at least 100,000 users whatever the scale. The OD matrix is less stable and depends on the scale with a share of at least 75% of commuters in common when considering all types of flows constructed from the home-work locations of 100,000 users. For both tasks, better results can be obtained at larger levels of aggregation or by considering more users. These results confirm that ICT data are very useful sources for the spatial analysis of urban systems, but that their reliability should in general be tested more thoroughly.

INTRODUCTION

Massive amounts of geolocalized data are passively and continuously produced by individuals when they use their mobile devices: smart phones, credit cards, GPSs, RFIDs or remote sensing devices. This deluge of digital footprints is growing at an extremely fast pace and represents an unprecedented opportunity for researchers, to address quantitatively challenging questions, in the hope of unveiling new insights on the dynamics of human societies. Many fields are concerned by the development of new techniques to handle these vast datasets, and range from applied mathematics, physics, to computer science, with plenty of applications to a variety of disciplines such as medicine, public health and social sciences for example.

Although data resulting from the use of information and communications technologies (ICT) have the advantage of large samples sizes (millions of observations), and high spatio-temporal resolution, they also raise new challenging issues. Some are technical and related to the storage, management and processing of these data [1], while others are methodological, such as the statistical validity of analysis performed on such data. For example, in the case of mobile phone data, researchers have often no control and limited information regarding the data collection process, which obviously deserves other purposes than scientific research.

Various hidden biases can affect these data used to study the spatial behavior of anonymized individuals, and consequently observing the world through the lenses of ICT data may therefore lead to possible distortions and erroneous conclusions [2]. It is thus crucial to perform statistical tests and to develop methods in order to assess the robustness of the results obtained with ICT data. In the research community that studies human mobility in urban contexts [3–6], efforts in this sense have been made in recent years, notably by cross-checking results [7] obtained with ICT data and with more traditional data sources [7–13]. These comparisons cover different topics, such as the analysis of daily mobility motifs [8], the distribution of population at different scales [7, 10], the estimation of commuting flows [7, 9, 11, 13], and the identification of land uses [7, 12]. However, the robustness of results to sample selection, scale or sample size has, up to our knowledge, never been studied so far.

In the following, we present two examples of such uncertainty analysis on higher-level spatial information extracted from mobile phone metadata, which were produced in Senegal in 2013 [14]. We concentrate on two information-retrieval tasks: first, we evaluate the uncertainty when inferring land use from the rhythms of human communication [15–19]; second, we quantify the uncertainty when identifying individuals' most visited locations [7, 12, 20, 21]. We conclude by mentioning possible future steps in order to assess more clearly the relevance of various ICT data sources for studying a variety of urban dynamics.

* Corresponding author: maxime.lenormand@irstea.fr

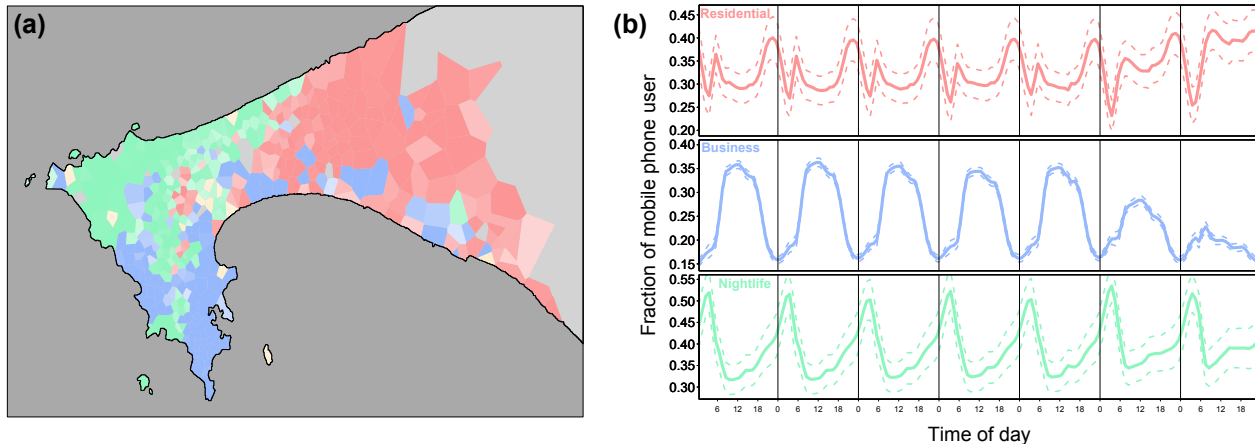


Figure 1. Spatio-temporal uncertainty propagation while inferring land use from mobile phone activity. (a) Map of the region of Dakar displaying the three clusters according to their land use. Colors vary from white to the most recurrent cluster identified in the random samples. The color saturation depends on the number of times the zone was classified as the most recurrent cluster. The color code is red for *Residential*, blue for *Business*, green for *Nightlife* and orange for other types of land use. (b) Temporal patterns associated with the three clusters. The solid lines represent the average temporal profile computed over the random extractions, while the dashed lines represent one standard deviation. These results were obtained at the Voronoi scale for 50 independent random extractions of 150,000 users mobile phone activity during one week.

STUDY AREA AND DATA DESCRIPTION

We focus here on the region of Dakar, Senegal. The mobile phone data consists in call detail records (CDR) of phone calls and short messages exchanged by more than 9 million of anonymized Orange’s customers. They were collected in Senegal in 2013, and were released to research teams in the framework of the 2014 Orange Data for Development challenge [14]. We use in this study the second dataset (SET2) that was made available by Orange, and which contains fine-grained location data on a rolling 2-week basis at the individual level. For each of the 25 two-weeks periods, a sample of about 300,000 mobile phone users were randomly selected at the country scale. Whenever one of these individuals uses his/her mobile phone during the two-week period, the time and his/her position (at the level of serving cell tower) are recorded. These information can be used to study human activity and mobility patterns in the region of Dakar, that is here divided into 457 zones. This spatial partition is the Voronoi tessellation constructed from the location of phone antennas in the city, chosen as nodes. Each Voronoi cell thus approximates the activity zone served by the antenna located at its center (see Figure S1a).

INFERRING LAND USE FROM MOBILE PHONE ACTIVITY

Functional network of the city

Geolocalized ICT data have been widely used to infer land use from human activity [15–19]. The basic idea is to divide the region of interest into zones,

extract a temporal activity signal for each of these zones, and then cluster together zones that display similar signals. Each of the resulting clusters then corresponds to a certain type of activity (*Residential*, *Commercial*, ...). We used here the functional approach proposed in [19]. This method takes as input, for each zone, a signal composed of 168 points ($24\text{h} \times 7\text{ days}$), each value corresponding to the number of users located in this zone, at this hour of the day, this day of the week. These signals are then normalized by the total hourly activity, in order to subtract trends introduced by circadian rhythms. A Pearson correlation matrix between zones is then computed. Two zones whose activity rhythms are strongly correlated in time will have a high positive correlation value. This similarity matrix can be represented by an undirected weighted network, which is then clustered using the *Infomap* community detection algorithm [22]. This method has the advantage to be non-parametric (the number of clusters is not fixed *a priori*).

Signal extraction and sampling strategy

In order to apply this functional approach to the region of Dakar, we first need to define a method for sampling and aggregating spatially the users’ mobile phone activity as extracted from the raw data. In this dataset, the mobile phone activity in Senegal during the year 2013 has been divided into 25 two-weeks periods that we separate into 50 time windows of one week. For each week, we build the users’ temporal mobile phone activity by relying on the following criteria: each individual counts only once per hour. If a user is detected in k different zones within a given

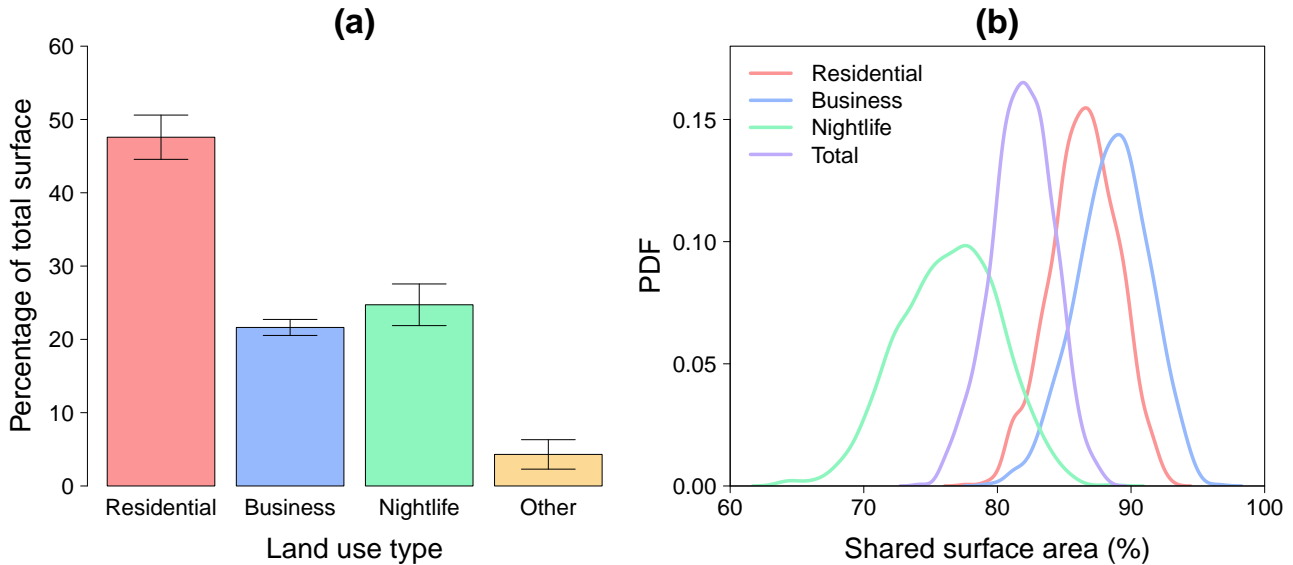


Figure 2. Uncertainty when inferring land use from mobile phone activity. (a) Area covered by the different land use types, expressed as a percentage of the total surface. The values have been averaged over 50 random extractions, and the error bars represent one standard deviation. (b) Probability density function of the shared surface area between each pair of spatial distributions according to the type of land use. These results were obtained at the scale of the mobile phone towers (Voronoi tessellation), and they are based on the comparison of 50×50 independent samples with 150,000 signals.

1-hour time period, each registered position will count as $(1/k)$ ‘units of activity’ for each of these k zones. It is important to note that only signals containing activity in the region of Dakar have been considered. At the end of the process, we obtain the temporal signal of about 160,000 users per week, a value that is quite stable over the 50 weeks. These temporal signals can then be averaged into a temporal signal of activity for each zone allowing us to identify different land use type in the region of Dakar by applying the above method. Note that since in the original dataset the year is divided into two-weeks periods and that a user could appear in two or more two-weeks periods, several signals of a same user (during different weeks) can be observed among the 50 weeks of activity.

We also need to define a sampling strategy for assessing the robustness of land use identification with respect to sample selection. In order to analyze and compare spatial distributions of land use obtained with different samples of individual temporal signals, we needed to ensure that these samples are independent (i.e. no signals in common) and also that they are evenly distributed across the entire year. For example, if we want to compare two spatial distributions of land use based on two independent samples composed of 150,000 signals (i.e. individuals) each, we will draw at random two independent samples of 3,000 signals (individuals) for each week. We will then spatially and temporally aggregate the signals over the 50 weeks in order to obtain two independent aggregate signals, each composed of $3,000 \times 50$ distinct individual signals. We then apply the functional approach described above for extracting the spatial partitions of land use, and for investigating the uncertainty of

these partitions to individuals’ sample selection. The influence of the sample size or the scale on the uncertainty can also be investigated by varying the number of signals for each random extraction, and/or by spatially aggregating them over spatial grids made of regular square of varying (parameterized) sizes.

Spatial propagation of uncertainty

As a first step, we applied the functional approach on 50 independent random extractions of 150,000 individual signals across the entire year, at the scale of the Voronoi cells (mobile phone towers locations), by using the sampling strategy described in the previous section. Three clusters of zones emerged systematically, covering on average 95% of the total surface. The remaining 5% correspond to other clusters with no clear patterns, probably associated with some local punctual events. We show on Figure 1b the average temporal profiles along with the variability around this average, for each of these three clusters. Each of the clusters can be roughly associated to a typical rhythm of human activity, and consequently to a characteristic land use:

- A *Residential* activity profile, corresponding to a high probability of mobile phone use during early mornings, evenings and week end days.
- A *Business* cluster, displaying a significantly higher activity from 9am to 5-6pm during week-days.
- A *Nightlife* activity profile, characterized by a high activity during night hours (1am-4am).

The *Nightlife* cluster (in green) covers the area of the international airport, and also the neighborhood of ‘*La Pointe des Almadies*’, where mainly wealthy people live and where are located most of the rich nightclubs. The *Business* cluster covers Dakar’s central business district (‘*Le Plateau*’), where one finds companies’ headquarters, and where the port is also located. Finally, the *Residential* cluster covers the rapidly growing parts of the Dakar peninsula, which profits from the highway construction. It is worth noting that the different land use types identified in this study are consistent with the ones obtained with another mobile phone dataset in Spain [19], except that in the case of Dakar, the method is not able to distinguish between industrial (or logistic) and leisure/nightlife activities (see [19] for more details).

As can be observed in Figure 2a, the area covered by the different types of land use is quite stable over the 50 samples, with the *Residential* land use type representing on average about 50% of the total surface, while we observe about 20% and 25% for the *Business* and *Nightlife* clusters, respectively. Nevertheless, the stability of the proportion does not imply that they follow the same spatial distribution from one sample to another. In order to test the stability, we computed the proportion of surface area shared by two spatial distributions p_l and p'_l of a given type l , as obtained with two different samples. The expression for this quantity is

$$S = 2 \frac{A_{p_l \cap p'_l}}{A_{p_l} + A_{p'_l}}, \quad (1)$$

where A_{p_l} denotes the surface area of spatial distribution p_l . Note that in our case $A_{p_l} \simeq A_{p'_l}$ (Figure 2a). Similarly, we can define the total surface area shared by two spatial partitions p and p' (with the same number and type of land use) of the region of interest,

$$S^* = \frac{\sum_l A_{p_l \cap p'_l}}{\sum_l A_{p_l}}. \quad (2)$$

The results are displayed in Figure 2b. The similarities between the 50 different spatial partitions is globally high, with on average 80% of shared surface area. The agreement is larger for the *Residential* and *Business* clusters with an average shared surface area around 90%, against 75% for the *Nightlife* land use type. This is probably due to the more episodic character of the nightlife activity, implying a smaller statistical reliability of the results. A map of the region of Dakar displaying the uncertainty associated with the land use identification is shown in Figure 1a. The colors represent the different land use types, and each zone has been assigned its recurrent cluster type over the 50 land use identifications. The color saturation is then related to the uncertainty, quantified by the number of times the zone was classified as a given recurrent cluster: the color is darker if the uncertainty is low, paler otherwise. Most of the zones have been

assigned to the same clusters more than 80% of the time.

Influence of scale and sample size on the uncertainty

The identification of land use from mobile phone activity seems to be quite robust to the sampling of individuals. So far we considered communication data of 150,000 users, available at their maximal spatial resolution, that is the locations of the mobile phone carrier’s antennas. But what about the influence of spatial scale and sample size on this uncertainty? In order to answer this question, we applied the same functional approach, but this time by (a) varying the number of individual signals of each random extraction (from 25,000 to 300,000, by step of 25,000) and (b) aggregating them spatially over spatial square grids with cells of side length equal to 1, 2 or 3 km (Figure S1) (the spatial aggregation is based on the area of the intersection between the Voronoi and the grid cell). We performed the comparison between 100 pairs of independent samples for different population sizes, and spatial resolutions/grid sizes. The results are shown in Figure 3.

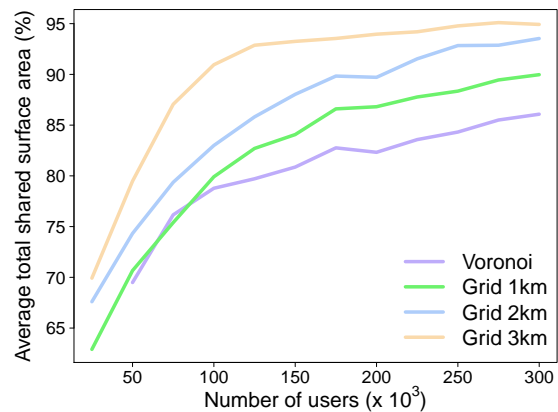


Figure 3. Influence of spatial scale and sample size. Total shared surface area S^* between land use partitions as a function of the sample size and for different spatial scales (Voronoi cells, and square grid cells of resp. 1, 2 and 3 km side length). In almost every case, the values displayed have been averaged over 100 independent comparisons. See Figure S3a for more details, while the full distributions are shown on Figure S2 in Appendix.

Interestingly, the *Nightlife* cluster does not systematically emerge, especially when considering small sample sizes at the ‘Voronoi scale’. In these cases, only two clusters are detected, the *Nightlife* activity cluster is mixed with *Residential* and *Business* activity clusters. As it can be observed in Figure S3 in Appendix, at least 100,000 individuals signals need to be aggregated to detect three clusters in more than 90% of the random sample extractions. This quantity falls down at 60% for sample population sizes of 75,000, about 15% for 50,000 and 0 for 25,000. We note that it never

happened when the signals have been spatially aggregated. Considering only the partitions for which three clusters were detected, we observe that the percentage of shared surface area increases when the data are spatially coarse-grained, and also with the number of individuals taken into account, revealing the existence of a typical scale. The order of this scale seems to be here of the order 100,000, above which we obtain more than 75% similarity between the land use spatial partitions. Coarse-graining the spatial resolution by projecting the data on grids of larger cells plays also an important role, allowing us to reduce the uncertainty when small samples are considered. As expected, the variability of the uncertainty tends to increase with the grid cell side length (see Figure S2 in Appendix).

Temporal variations

We considered so far samples uniformly distributed across the entire year, but comparisons of samples extracted from different time windows (i.e. communication activity recorded at different periods of the year) can also be performed in order to identify potential temporal variations. We therefore considered 12 consecutive time windows of four weeks (from the first week of January to the last week of November). For each possible pair of time-windows, we performed comparisons between 100 pairs of independent samples, each constituted of 150,000 signals (at the Voronoi scale). Figure 4 shows the average shared surface area, standardized by the average shared surface area across the entire year.

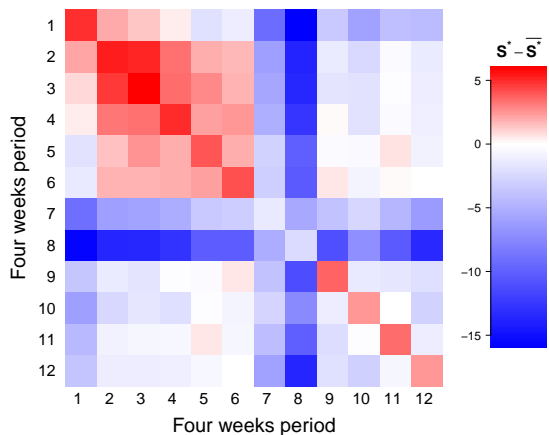


Figure 4. Temporal variations. Standard shared surface area between spatial partitions of land use extracted for different time windows (four weeks periods, from the first week of January to the last week of November). The standardization is performed by subtracting the average shared surface area obtained by comparing 50 independent samples based on 150,000 signals drawn at random across the entire year (Figure 2b). The values have been averaged over 100 independent comparisons based on 150,000 signals obtained at the Voronoi scale.

We observe that, in most cases, the shared surface

area is close to the one obtained on average for the entire year. As expected it is globally lower for the comparisons inside the same time window, and higher for the comparisons of partitions extracted for distinct time windows. It is also worth noting that similarity between time periods decreases with the time elapsed between them, and that the land use patterns identified in the first half of the year seems to be more similar than the ones observed in the second half of the year. It is however not clear whether these changes are due to changes in the city structure itself, or to seasonal variations. The most unexpected result is the change of behavior observed in summer during the weeks 7 and 8 (from the end of June to the middle of August) showing a similarity always lower than the average, -15 points in the worst case. This can be explained by the change of activity generally observed in summer. This information should be nevertheless taken into account when analyzing this type of data.

IDENTIFYING HOME AND WORK LOCATIONS FROM MOBILE PHONE ACTIVITY

Extracting individuals' most visited locations

Geolocalized ICT data are also widely used to identify the most visited locations of an individual, allowing to extract the origin-destination (OD) matrices of commuting flows, a fundamental object in mobility studies. A very simple heuristic used in most methods is the following: the most visited place of an individual in the late afternoon/evening and in the early morning is used as a proxy for his/her place of residence, while the most visited location during working hours is a proxy for his/her workplace (or main activity place). This simple assumption has allowed the accurate determination of mobility flows at intermediate geographical scales for a variety of cities worldwide (see for example [7, 9, 11, 12]). However, the robustness of the results obtained with such a simple heuristic, with respect to sample selection, has never been investigated.

For each of the 25 two-weeks periods and for each user, we apply the following procedure to extract the home and work locations:

- First, the hours of activity are divided into two groups, daytime hours (between 8am and 5pm included) and nighttime hours (between 7pm and 7am included). Only days of the week from Monday to Thursday are taken into account, that is to say 8 days in total over two weeks.
- We then apply a **first filter** by considering only users who were active at least N_d days (out of 8) during daytime **and** N_d days during night time.
- A **second filter** is then applied to keep only users who have been 'active', in total during the two weeks, at least N_h 1-hour periods during

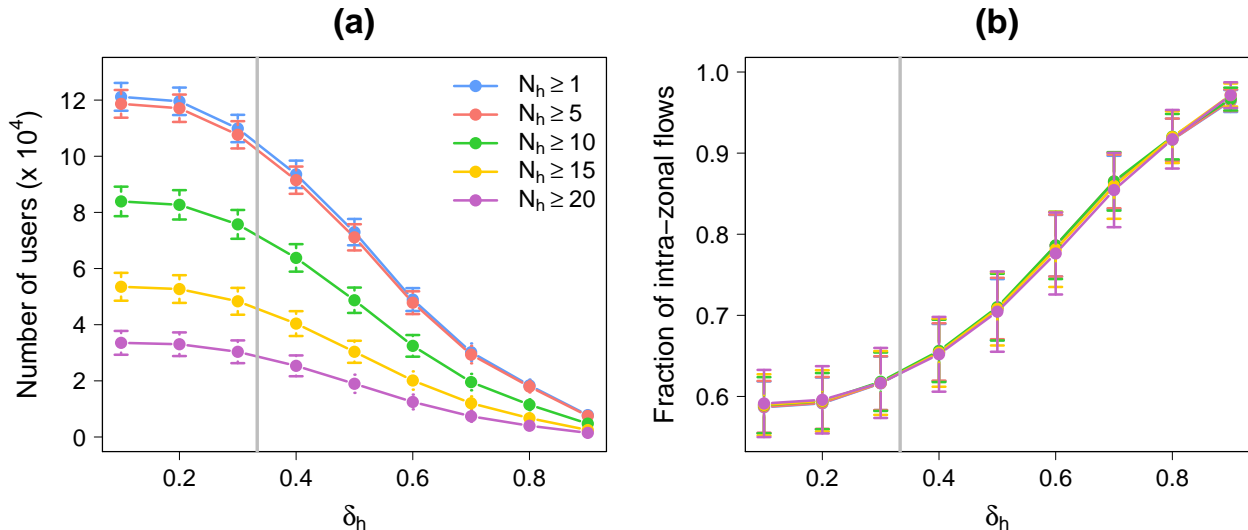


Figure 5. Influence of the parameters. Number of reliable users (a) and fraction of users living and working in the same zone (b) as a function of δ_h and for different values of N_h ($N_d = 4$). Only people living and working in the region of Dakar have been considered here. These results have been averaged over the 25 two-weeks periods, and error bars represent one standard deviation. The vertical bars indicate the value $\delta = 1/3$. Similar plots for different value of N_d ranging from 1 to 8 are shown in Figures S4 and S5 in the Appendix.

daytime, and N_h 1-hour periods during nighttime.

- For each hour of activity, the most frequently visited zone during this hour is identified (based on his/her geolocalized mobile phone activity).
- For both groups of hours (daytime and nighttime), we identify the zone in which the user has been localized the highest number of hours.
- A **third and last filter** is also implemented to select only users whose fraction of hours spent at ‘home’ and ‘work’ are larger than a fraction δ_h of the total number of locations visited during nighttime and daytime, respectively.
- Finally, only individuals living and working in the region of Dakar are considered as reliable users.

The last filter allow us to adjust the degree of confidence in the identification of the main nighttime (‘Home’) and daytime activity (‘Work’) locations. A low value of δ_h allows us to maximize the number of reliable users (Figure 5a), with the risk of including places of main activity where the user has spent very little time. On the contrary, a high value of δ_h will make us keep only users moving very little during nighttime and/or daytime, and who therefore may not be representative of the variety of mobility patterns at a small scale. As it can be observed in Figure 5b, these users are generally people living and working in the same area. Based on these considerations, we chose to fix δ_h to $1/3$ which seems to be a good interplay, allowing us to remove users exhibiting irregular mobility patterns during the time period, while preserving the commuting network structure in the Dakar region.

The behavior of δ_h on the number of reliable users and the fraction of intra-zonal flows (users living and working in the same area) is independent of N_h and N_d (see Figures S4 and S5). These two first filters are applied to discard users having a mobile phone activity that is too low, and/or not sufficiently staggered over the two-weeks period. Two time scales have been considered, N_h for the hours and N_d for the days. The goal is to combine these two parameters to select users having a significant number of hours ‘in activity’ spread over a number of days large enough to guaranty the reliability of the information provided by the most visited locations extraction process. We were not able to identify any criteria for calibrating these two parameters, and we have therefore decided to fix the value of N_d to 4 days (half of the time period) and the value of N_h to 12 hours. Combined with a value of $\delta_h = 1/3$, this results in keeping around 50,000 reliable users for each two-weeks period (Figure 5a). Later, we will analyze more systematically how the value of N_h impact the uncertainty in the OD estimation and its topological structure.

The source code used to extract most visited locations from individual spatio-temporal trajectories is available online [23].

Sampling strategy and similarity metrics

Sampling strategy

Similarly to the land use identification, we need a sampling strategy for assessing the robustness of the OD extracted with respect to the sample selection, and we use independent samples of equal sizes drawn

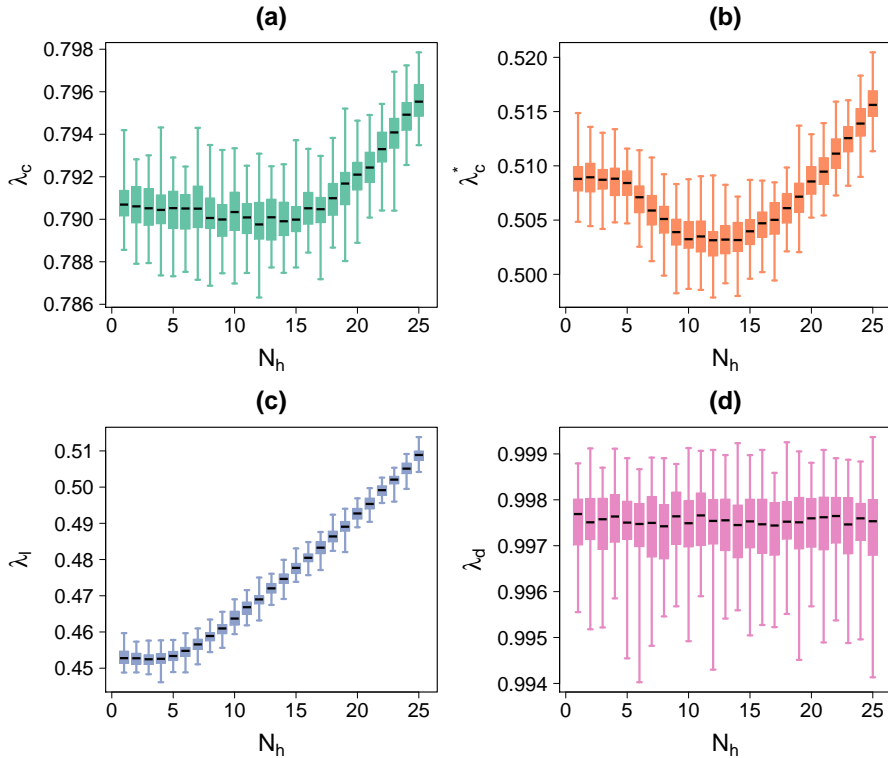


Figure 6. Uncertainty when inferring home-work locations from mobile phone activity. Boxplots of the comparisons between 100 independent ODs according to N_h . (a) λ_c (all flows). (b) λ_c^* (only inter-zonal flows). (c) λ_l . (d) λ_d . ODs have been extracted at the Voronoi scale from independent samples composed of 150,000 reliable users' home-work locations (with $N_d = 4$ and $\delta_h = 1/3$). The whiskers correspond to the minimum and maximum of the distributions.

at random across the 25 two-weeks periods. For example, for comparing two ODs retrieved from two independent samples of 150,000 reliable users' home-work locations, we draw at random two independent samples of size 6,000 for each of the two-weeks period. Here also, we evaluate the influence of the sample size and of the spatial resolution on the uncertainty, by varying the number of signals extracted at each random extraction and/or by spatially aggregating the signals over spatial grids of varying sizes.

Similarity metrics

The resulting commuting networks can be compared using several similarity metrics, such as the one described in [24]. We consider two commuting networks T and T' , where T_{ij} is the number of users living in zone i and working in zone j , and we will use three different metrics, that encode different network properties. First, the common fraction of commuters, noted λ_c , varying from 0 (when there is no overlap) to 1 (when the two networks are identical) is given by

$$\lambda_c = \frac{2 \sum_{i,j} \min(T_{ij}, T'_{ij})}{\sum_{i,j} T_{ij} + \sum_{i,j} T'_{ij}}. \quad (3)$$

With this first metric, the similarity is calculated considering all flows, without distinction between the

intra-zonal flows and the inter-zonal flows. The first type of flows tends to gather a large part of the commuters distributed over a limited number of links whereas the latter are usually less stable and more difficult to estimate. To take into consideration these different types of flows we will also consider, as a similarity metric, the common fraction of commuters, λ_c^* , based only on the users living and working in two different places ($i \neq j$).

Second, we will consider the common fraction of links, λ_l , that measures similarity in the networks' topological structure, and is calculated as

$$\lambda_l = \frac{2 \sum_{i,j} \mathbb{1}_{T_{ij}>0} \cdot \mathbb{1}_{T'_{ij}>0}}{\sum_{i,j} \mathbb{1}_{T_{ij}>0} + \sum_{i,j} \mathbb{1}_{T'_{ij}>0}}. \quad (4)$$

Third, we measure the common share of commuters according to the distance, λ_d , assessing the similarity between commuting distance distributions and given by

$$\lambda_d = \frac{\sum_k \min(N_k, N'_k)}{N}, \quad (5)$$

where N_k stands for the number of users with a commuting distance ranging between $2k - 2$ and $2k$ kms (k ranging from 1 to ∞) and N for the total number of users.

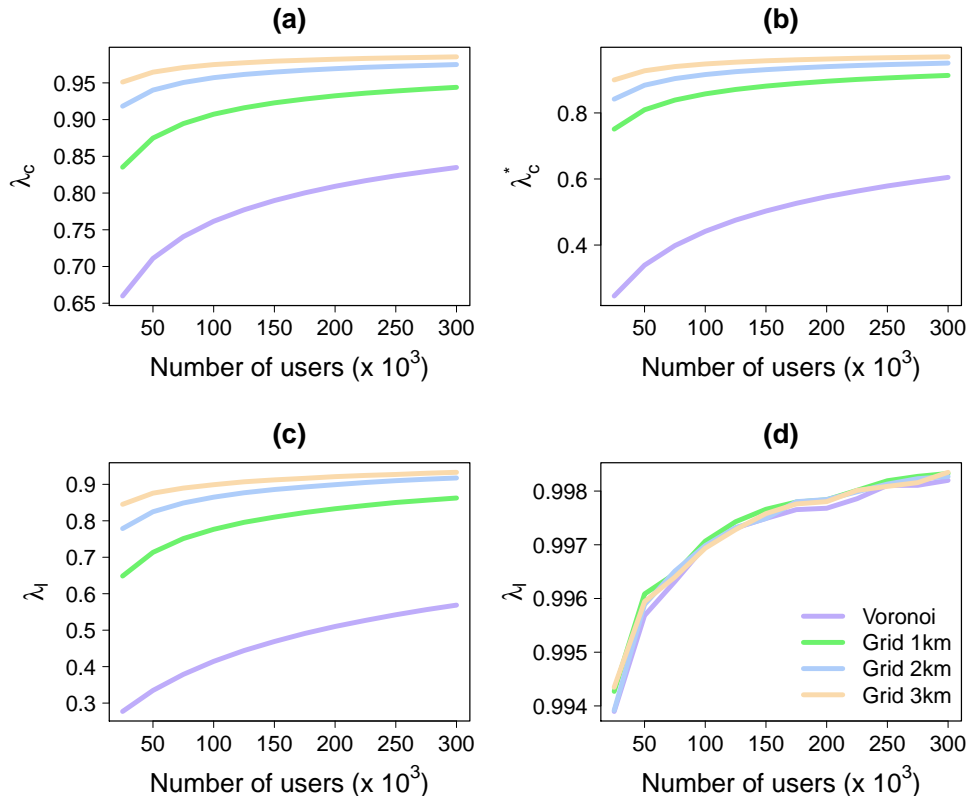


Figure 7. Influence of spatial scale and sample size. Similarity metrics as a function of the sample size, according to various spatial scales (Voronoi cells and regular square grid of cells of 1, 2 and 3 km side length). (a) λ_c (all flows). (b) λ_c^* (only inter-zonal flows). (c) λ_l . (d) λ_d . The values displayed have been averaged over 100 independent comparisons with $N_d = 4$, $N_h = 12$ and $\delta_h = 1/3$. The same figure displaying the full distribution instead of the average is available in Figure S7 in Appendix.

Uncertainty analysis

Boxplots of the similarity metric values obtained by comparing 100 independent ODs based on 150,000 reliable users' home-work locations are displayed in Figure 6. We first concentrate on the influence of N_h on the uncertainty and on the networks' topological structure, and we observe that the only metrics really affected by the number of hours of activity is the share of links λ_l , which increases linearly with N_h . This is an expected behavior since the constraint on the number of hours in activity selects the most regular individuals and reduces the noise, decreases the number of links, and coherently produces more robust ODs. The effect of N_h on the other similarity metrics is quite negligible, particularly on the similarity between commuting distance distributions λ_d . The values of λ_c and λ_c^* move up and down with the number of links (Figure S6 in Appendix) but the fluctuations stay reasonably small, 0.01 point for the λ_c and 0.02 point for λ_c^* . The fact that the number of links increases for values of N_h ranging from 5 to 15 is not trivial (Figure S6 in Appendix). It is even more surprising to see that this increase is due to the growth of the number of links of small sizes (between 2 and 10 commuters) that are not able to counterbalance

the falls of the number of very small (1 user) and big links (more than 10 users). These changes of network structure are not easy to understand and would probably necessitate more information about commuting in Senegal to be investigated more thoroughly.

Regarding the uncertainty, the results are not completely conclusive, the commuting networks show a good agreement with around 79% of commuters in common (considering both inter- and intra-zonal flows), but with a value that falls down to 50% when only inter-zonal flows are considered. This decrease of similarity can be explain by the fact that intra-zonal flows represent 60% of the commuters distributed on a number of links that is bounded by the number of zones, whereas inter-zonal flows are generally smaller since they represent less commuters distributed on a higher number of links. This is why when we remove the intra-zonal flows which are usually easier to estimate, we increase the uncertainty. The λ_l values are also quite low, between 45% and 51% of links are in common between the different networks according to the value of N_h . An encouraging result is that the common part of commuters according to the distance is very high, showing around 99% of similarity between the commuting distance distributions. However, it is important to keep in mind that these mixed

results are obtained with a few thousand users for each two-weeks commuting network, drawn at a high spatial resolution with an average surface area equal to 0.5 km^2 .

Influence of scale and sample size

The effect of the spatial resolution and sample sizes on the similarity metrics can be investigated by varying the number of reliable users' home-work most visited locations to build the ODs and/or by aggregating them spatially using grid cells of different sizes (see [7] for more details about the aggregation method based on the area of the intersection between the Voronoi and the grid cells). As it can be observed in Figure 7, increasing the sample size and/or the scale greatly improve the results. Here again, considering at least 100,000 reliable users seems to be a good trade-off and ensure a common part of commuters larger than 75%. The most significant improvement comes from the spatial aggregation, which at least double λ_c^* and λ_l values and allow us to obtain λ_c values almost always larger than 0.85. There is one exception, though, with λ_l that seems to be independent from the spatial aggregation scale used.

Temporal variations

The effect of temporal variations on the uncertainty of OD estimates can be investigated by considering 12 consecutive time windows of four weeks (from the first week of January to the last week of November, see section on land use detection). In this case, ODs are based on 50,000 reliable users' home-work most visited locations, determined at the Voronoi scale. The similarity metrics have been standardized by subtracting the average metrics values across the entire year. Figure 8 shows the results obtained with the common part of commuters λ_c (similar results obtained with the other metrics are shown on Figure S8 in Appendix). As in the case of land use identification, the values are close to the average, lower for the inter time windows comparisons than for the intra comparisons. We also observe that the results are more stable after summer holidays, during the second half of the year. An evolution of the commuting networks over time can be observed with a decrease of the similarity metrics values as the time elapsed between time periods increases.

Sampling of points along individual trajectories

In order to go further, for each of the 25 two-weeks periods and for each user, we identified the home and work locations for each of the two weeks considered independently, by following the procedure described above with $N_d = 2$ (half of the time window) and

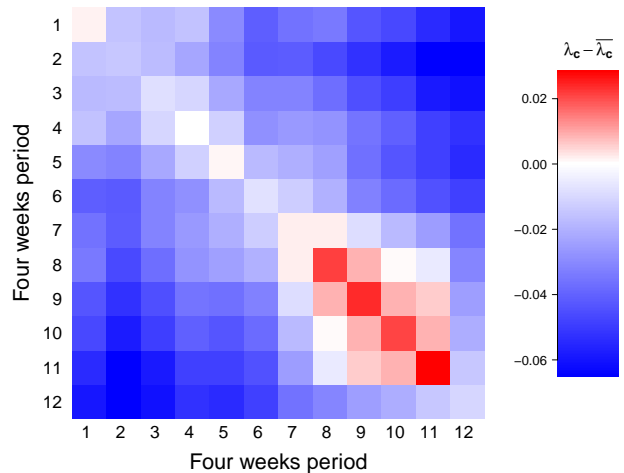


Figure 8. Temporal variations. Standard λ_c between ODs extracted for different time windows (four weeks periods, from the first week of January to the last week of November). The standardization has been obtained by subtracting the average λ_c obtained by comparing 100 independent samples based on 50,000 reliable users' home-work most visited locations drawn at random across the entire year. The results have been averaged over 100 independent comparisons based on 50,000 reliable users' home-work most visited locations at the Voronoi scale. Plots of the other similarity metrics are available in Figure S8 in Appendix.

$\delta_h = 1/3$. This allowed us to assess the influence of the sampling of points along individual trajectories when identifying the home and work locations. We then compared the locations identified for each of the two-weeks period according to the value of N_h . While the effect of N_h on the level of accuracy is quite low, it is however important to note that the level of accuracy in the estimate of home location tends to increase with N_h . Considering the high spatial resolution and the small time window, a good agreement is obtained, with an accuracy of around 84% for home (average over the 25 two-week periods) and 78% for work (Figure 9). Moreover, 50% of the inaccurate locations are less than 2 kms distant from each other. We can therefore conclude that the identification of users' home and work locations from mobile phone activity also shows a high level of robustness to sample selection.

DISCUSSION

Data passively produced through information and communications technologies have been increasingly used by researchers since the middle of the 2000's and our understanding of number of aspects of human mobility has already been deeply renewed thanks to these new data sources. More generally, the longitudinal tracking of anonymized individuals opens the door to an enhanced understanding of social phenomena that could not be studied empirically at such scales before. However, these data obviously suffer from a number of biases [2], which include in particular sample selec-

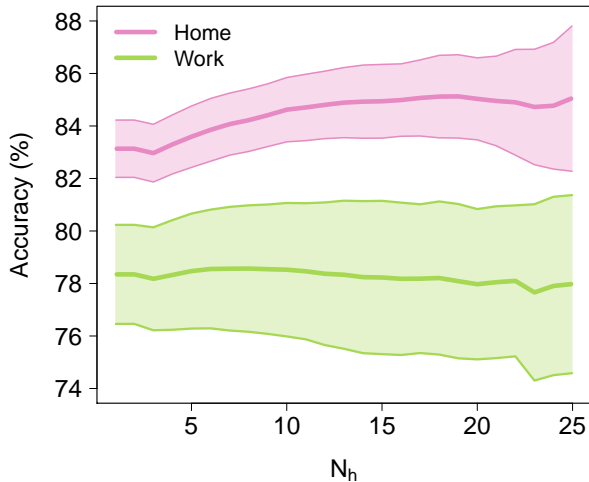


Figure 9. Percentage of accuracy in home and work locations' estimation according to N_h . Results have been averaged over the 25 two-weeks time windows. The thin lines represent one standard deviation.

tion. Systematic tests are then required to characterize statistical validity, along with cross-checks between various data sources.

This in mind, we performed two uncertainty analysis of results obtained with mobile phone data produced by millions of anonymized individuals during an entire year. In the first part of the analysis, we assessed the uncertainty when inferring land use from human activity, estimated from the number of mobile phone users present in different parts of the city, at different moments of the week. A good agreement was obtained between land uses identified from independent and randomly selected samples of individuals mobile phone activity during one week. We showed that samples should be composed of at least 100,000 individual signals of activity in order to ensure that there is at least 75% of shared surface area between the spatial partitions of land uses automatically retrieved, whatever the level of spatial aggregation of the data. In the second part of the analysis, we investigated the influence of sample selection on the identification of users' home and work locations. We first examined the impact of the selection of users on the journey-to-work commuting networks extracted at the city scale. In our case-study of the city of Dakar, we showed that the level of uncertainty is largely dependent on the spatio-temporal resolution, and that good results were reachable with a reasonable level of spatial aggregation. We then analyzed the effect of the sampling of locations along mobile phone users' tra-

jectories on the identification of their home and work locations. Most of the locations identified with different samples were the same, or very close to one another. Finally, we also showed that in both cases the uncertainty varies according to the period of the year at which the data were gathered, particularly in summer for the land use identification.

A useful and natural extension to this work would be to compare the results obtained in this study with traditional mobility data sources such as surveys or census data, particularly to calibrate the parameters of the home-work most visited location identification process. It was unfortunately not possible to obtain such data from the Senegal census, but this type of analysis should be done whenever possible.

For these two spatial information retrieval tasks, our results suggest that the level of uncertainty associated with sample selection is globally low. Further work in this direction include the reproduction of such uncertainty analysis with other datasets coming from different countries and data sources. An important aspect of the rapidly growing 'new science of cities' [25], which heavily relies on new data sources, is to be able to reproduce results with different datasets, and to characterize and control to what extent the information provided by different sources are biased in a particular direction.

More studies in this spirit need to be done to strengthen the foundations of the field dedicated to the understanding of urban mobility and urban dynamics through ICT data. From a publication point of view, trying to reproduce previous results with different data sources, or to estimate the robustness of previously published results, might not be as appealing as proposing new measures and models, but is crucially important as well. As part of that work, we developed a collaborative website [26] where we give references for papers and datasets dealing with ICT data accuracy.

ACKNOWLEDGMENTS

Partial financial support has been received from the Spanish Ministry of Economy (MINECO) and FEDER (EU) under project ESOTECOS (FIS2015-63628-C2-2-R), and from the EU Commission through project INSIGHT. The work of TL has been funded under the PD/004/2015, from the Conselleria de Educaci3n, Cultura y Universidades of the Government of the Balearic Islands and from the European Social Fund through the Balearic Islands ESF operational program for 2013-2017.

[1] S. Kaisler, F. Armour, J. A. Espinosa, and W. Money. Big Data: Issues and Challenges Moving Forward. In *2014 47th Hawaii International Conference on System Sciences*, volume 0, pages 995–1004, 2013.

[2] K. Lewis. Three fallacies of digital footprints. *Big Data & Society*, 2(2), 2015.

[3] C. Ratti, D. Frenchman, Riccardo M. Pulselli, and S. Williams. Mobile landscapes: using location data

- from cell phones for urban analysis. *Environment and Planning B: Planning and Design*, 33(5):727–748, 2006.
- [4] T. Louail, M. Lenormand, O. G. Cantu, M. Picornell, R. Herranz, E. Frías-Martínez, J. J. Ramasco, and M. Barthelemy. From mobile phone data to the spatial structure of cities. *Scientific reports*, 4, 2014.
- [5] F. Calabrese, L. Ferrari, and V. D Blondel. Urban sensing using mobile phone network data: a survey of research. *ACM Computing Surveys (CSUR)*, 47(2):25, 2015.
- [6] T. Louail, M. Lenormand, M. Picornell, O. G. Cantú, R. Herranz, E. Frías-Martínez, J. J. Ramasco, and M. Barthelemy. Uncovering the spatial structure of mobility networks. *Nature Communications*, 6, 2015.
- [7] M. Lenormand, M. Picornell, O. G. Cantú-Ros, A. Tugores, T. Louail, R. Herranz, M. Barthelemy, E. Frías-Martínez, and J. J. Ramasco. Cross-Checking Different Sources of Mobility Information. *PLoS ONE*, 9(8):e105184, 2014.
- [8] C. M. Schneider, V. Belik, T. Couronné, Z. Smoreda, and M. C. González. Unravelling daily human mobility motifs. *Journal of The Royal Society Interface*, 10(84):20130246, 2013.
- [9] M. Tizzoni, P. Bajardi, A. Decuyper, G. K. K. King, C. M. Schneider, V. Blondel, Z. Smoreda, M. C. González, and V. Colizza. On the Use of Human Mobility Proxies for Modeling Epidemics. *PLOS Comput Biol*, 10(7):e1003716, 2014.
- [10] P. Deville, C. Linard, S. Martin, M. Gilbert, F. R. Stevens, A. E. Gaughan, V. D. Blondel, and A. J. Tatem. Dynamic population mapping using mobile phone data. *Proceedings of the National Academy of Sciences*, 111(45):15888–15893, 2014.
- [11] L. Alexander, S. Jiang, M. Murga, and M. C. González. Origin–destination trips by purpose and time of day inferred from mobile phone data. *Transportation Research Part C: Emerging Technologies*, 58, Part B:240–250, 2015.
- [12] J. L. Toole, S. Colak, B. Sturt, L. P. Alexander, A. Evsukoff, and M. C. González. The path most traveled: Travel demand estimation using big data resources. *Transportation Research Part C: Emerging Technologies*, 58, Part B:162–177, 2015.
- [13] S. Jiang, Y. Yang, S. Gupta, D. Veneziano, S. Athavale, and M. C. González. The TimeGeo modeling framework for urban motility without travel surveys. *Proceedings of the National Academy of Sciences*, page 201524261, 2016.
- [14] Y.-A. de Montjoye, Z. Smoreda, R. Trinquart, C. Ziemlicki, and V. D. Blondel. D4D-Senegal: The Second Mobile Phone Data for Development Challenge. *arXiv preprint*, arXiv:1407.4885, 2014.
- [15] V. Soto and E. Frías-Martínez. Automated land use identification using cell-phone records. In *Proceedings of the 3rd ACM international workshop on MobiArch, HotPlanet '11*, pages 17–22, New York, NY, USA, 2011. ACM.
- [16] V. Frías-Martínez, V. Soto, H. Hohwald, and E. Frías-Martínez. Characterizing urban landscapes using geolocated tweets. In *SocialCom/PASSAT*, pages 239–248. IEEE, 2012.
- [17] J. L. Toole, M. Ulm, M. C. González, and D. Bauer. Inferring Land Use from Mobile Phone Activity. In *Proceedings of the ACM SIGKDD International Workshop on Urban Computing, UrbComp '12*, pages 1–8, New York, NY, USA, 2012. ACM.
- [18] T. Pei, S. Sobolevsky, C. Ratti, S. L. Shaw, and C. Zhou. A new insight into land use classification based on aggregated mobile phone data. *International Journal of Geographical Information Science*, 28:1988–2007, 2014.
- [19] M. Lenormand, M. Picornell, O. Garcia Cantú, A. Tugores, T. Louail, R. Herranz, M. Barthelemy, E. Frías-Martínez, and J. J. Ramasco. Comparing and modeling land use organization in cities. *Royal Society Open Science*, 2:150459, 2015.
- [20] R. Ahas, Olle Silm, S. and J., E. Saluveer, and M. Tiru. Using Mobile Positioning Data to Model Locations Meaningful to Users of Mobile Phones. *Journal of Urban Technology*, 17(1):3–27, 2010.
- [21] S. Isaacman, R. Becker, R. Cáceres, S. Kobourov, M. t Martonosi, J. Rowland, and A. Varshavsky. Identifying Important Places in People’s Lives from Cellular Network Data. In Kent Lyons, Jeffrey Hightower, and Elaine M. Huang, editors, *Pervasive Computing*. Springer Berlin Heidelberg, 2011.
- [22] M. Rosvall and C. T. Bergstrom. Maps of random walks on complex networks reveal community structure. *Proceedings of the National Academy of Sciences*, 105(4):1118–1123, 2008.
- [23] <https://github.com/maximelenormand/Most-frequented-locations>.
- [24] M. Lenormand, A. Bassolas, and J. J. Ramasco. Systematic comparison of trip distribution laws and models. *Journal of Transport Geography*, 51:158–169, 2016.
- [25] M. Batty. *The New Science of Cities*. MIT Press, 2013.
- [26] <https://ictdataaccuracy.github.io>.

APPENDIX

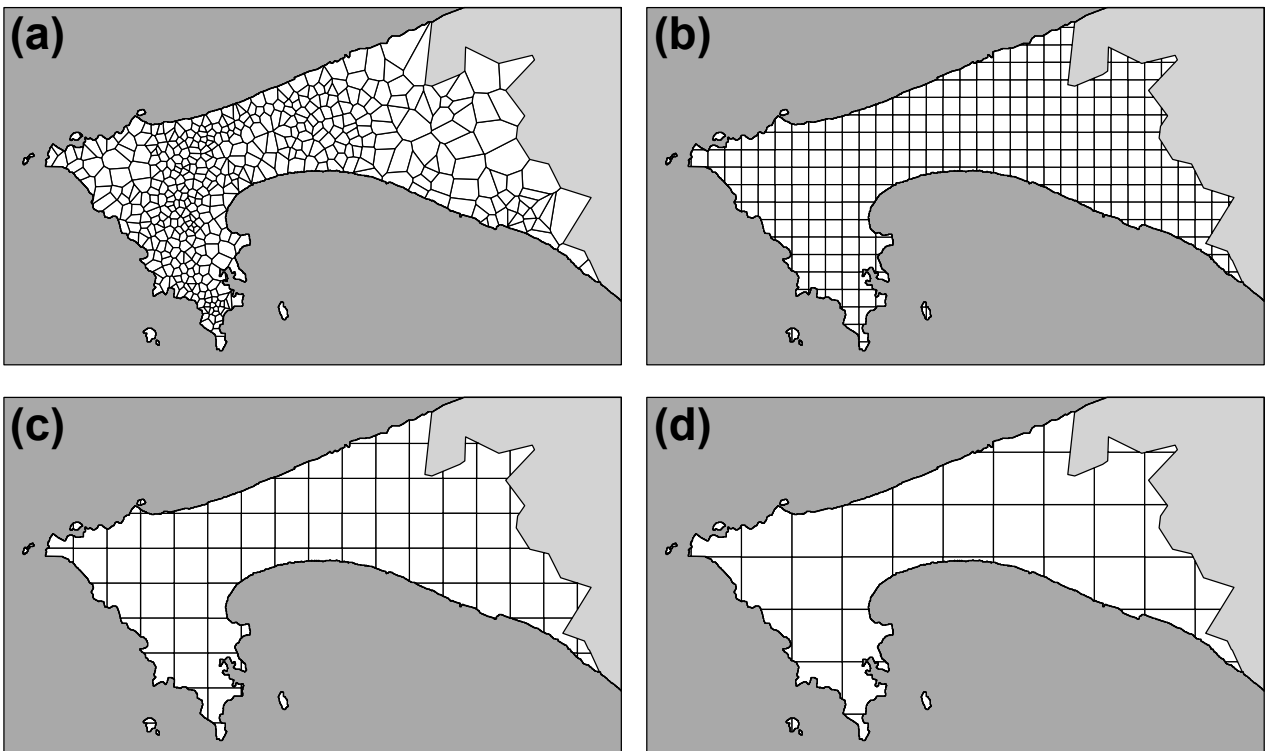


Figure S1. Map of the Dakar region. The white area represents the region of interest and the dark gray area represents the sea. Three scales of geographic units are represented. (a) Voronoi cells. (b) Grid cells ($1 \times 1 \text{ km}^2$). (c) Grid cells ($2 \times 2 \text{ km}^2$). (d) Grid cells ($3 \times 3 \text{ km}^2$).

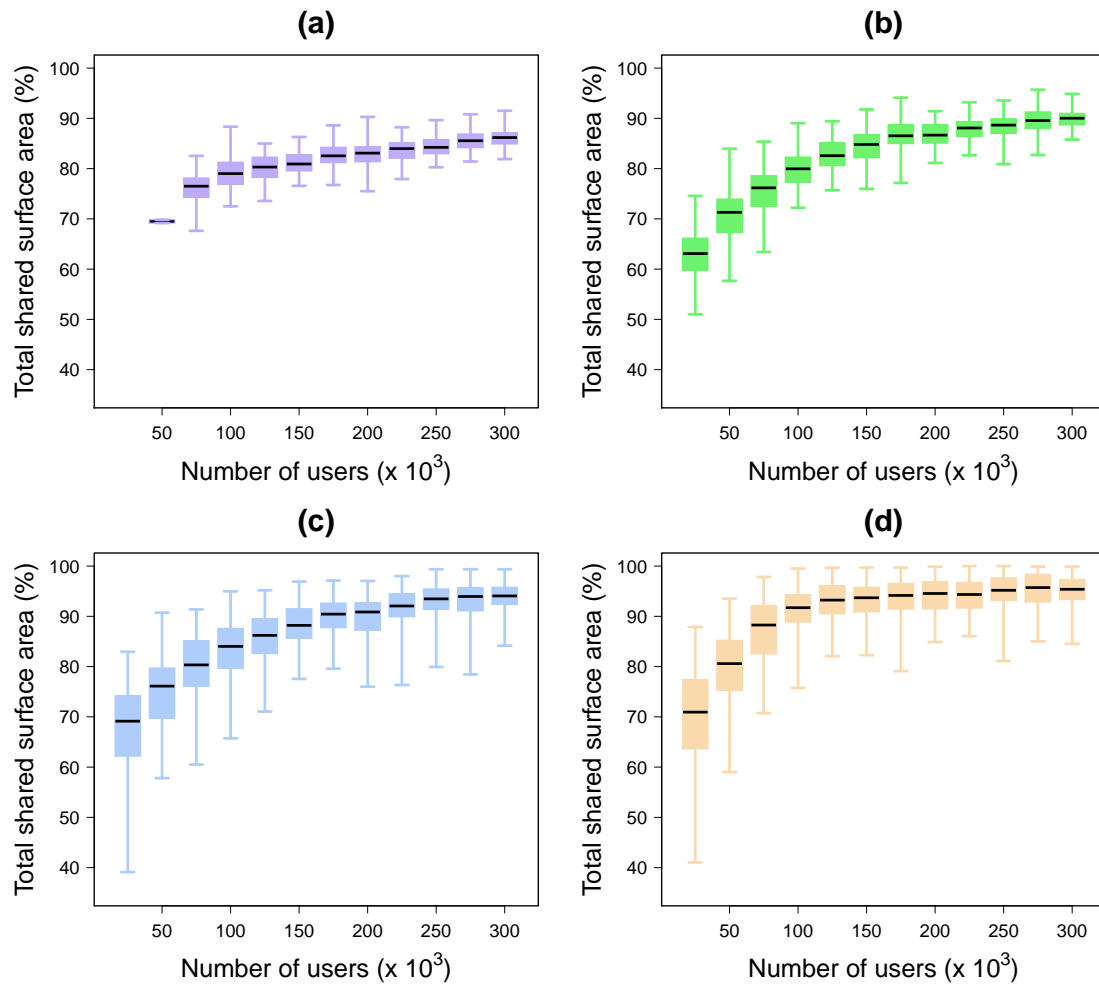


Figure S2. Influence of scale and sample size. Boxplots of the total share surface area as a function of the sample size according to the spatial scale. (a) Voronoi cells. (b) Grid cells ($1 \times 1 \text{ km}^2$). (c) Grid cells ($2 \times 2 \text{ km}^2$). (d) Grid cells ($3 \times 3 \text{ km}^2$). These results are based on 100 independent comparisons. The whiskers correspond to the minimum and maximum of the distributions.

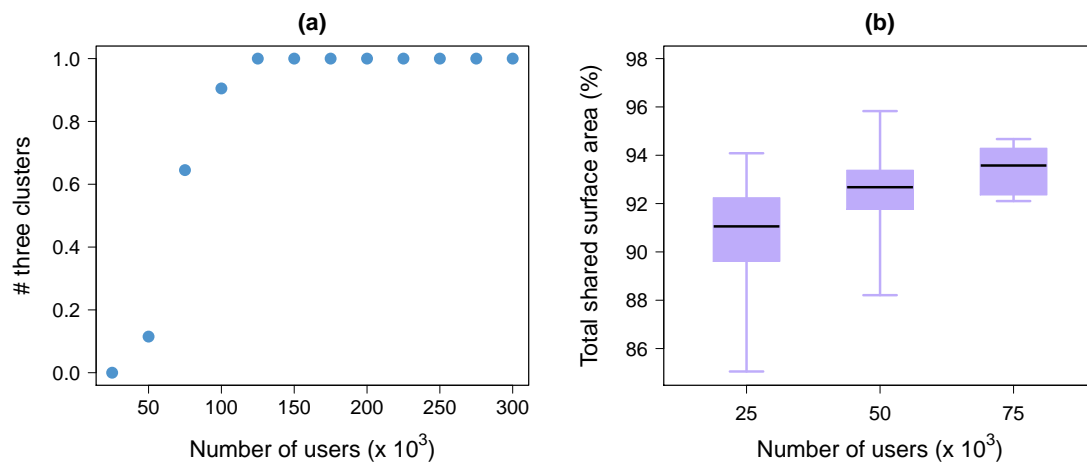


Figure S3. Influence of the sample size (at the Voronoi scale) on the number of clusters. (a) Fraction of random extractions for which three clusters were detected. (b) Boxplots of the share surface area for comparisons for which the number of clusters detected in the two independent samples were two. The whiskers correspond to the minimum and maximum of the distributions.

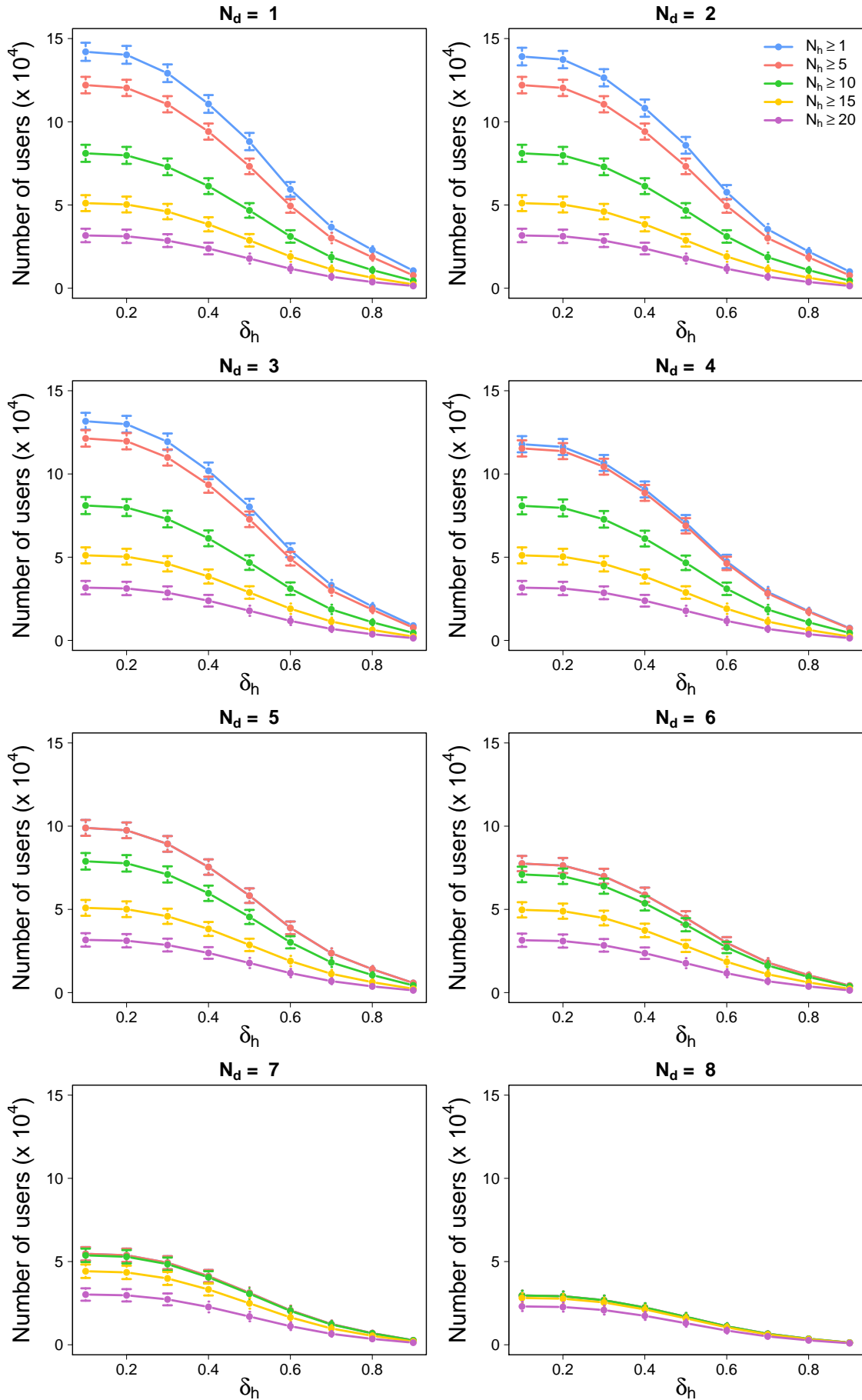


Figure S4. Influence of the parameters on the number of reliable users. Number of reliable users as a function of δ_h and according to N_h and N_d . Only people living and working in the region of Dakar have been considered. The values have been averaged over the 25 weeks, and the error bars represent the standard deviation.

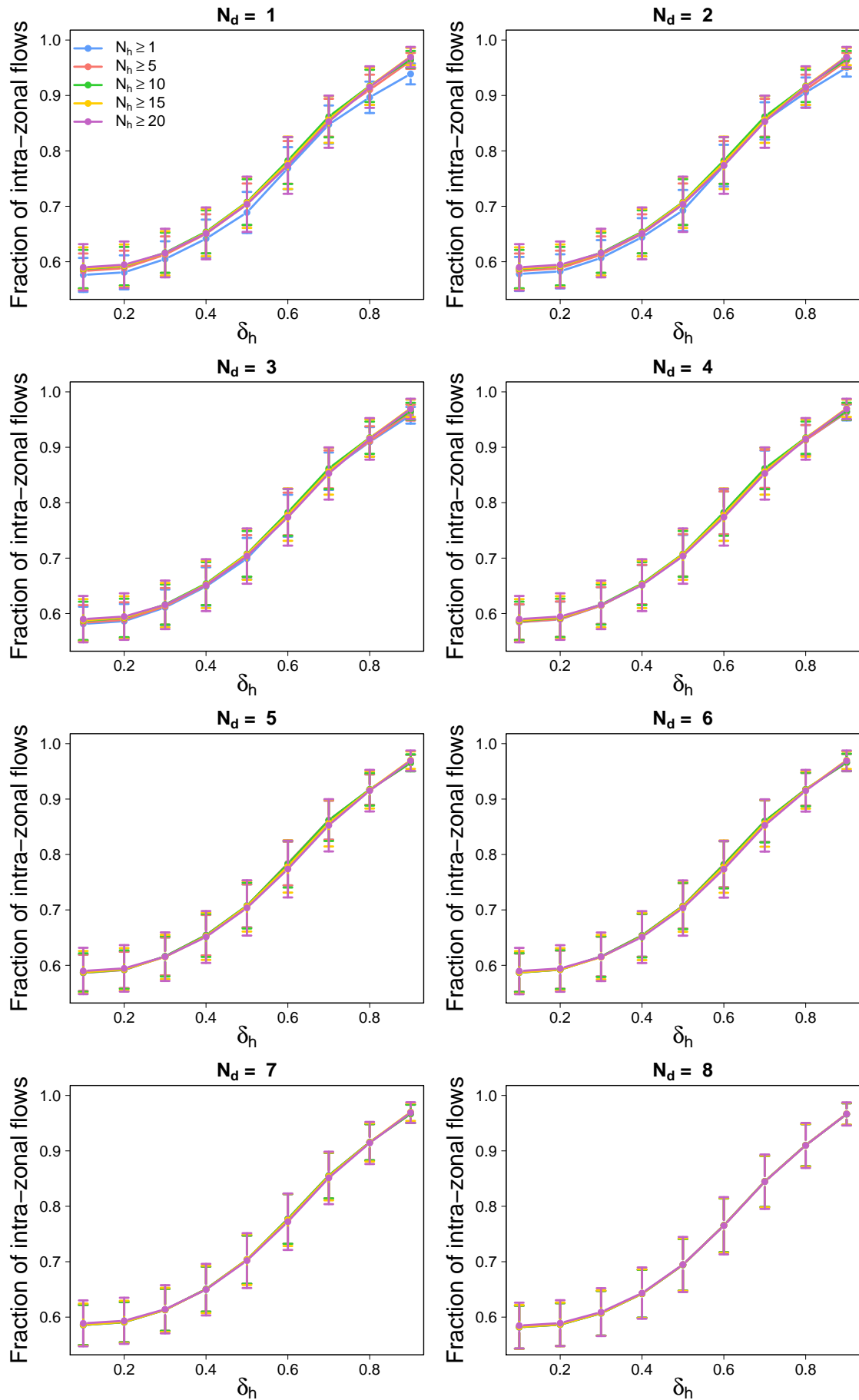


Figure S5. Influence of the parameters on the fraction of intra-zonal flows. Fraction of users living and working in the same zone as a function of δ_h and according to N_h and N_d . Only people living and working in the region of Dakar have been considered. The values have been averaged over the 25 weeks, and the error bars represent the standard deviation.

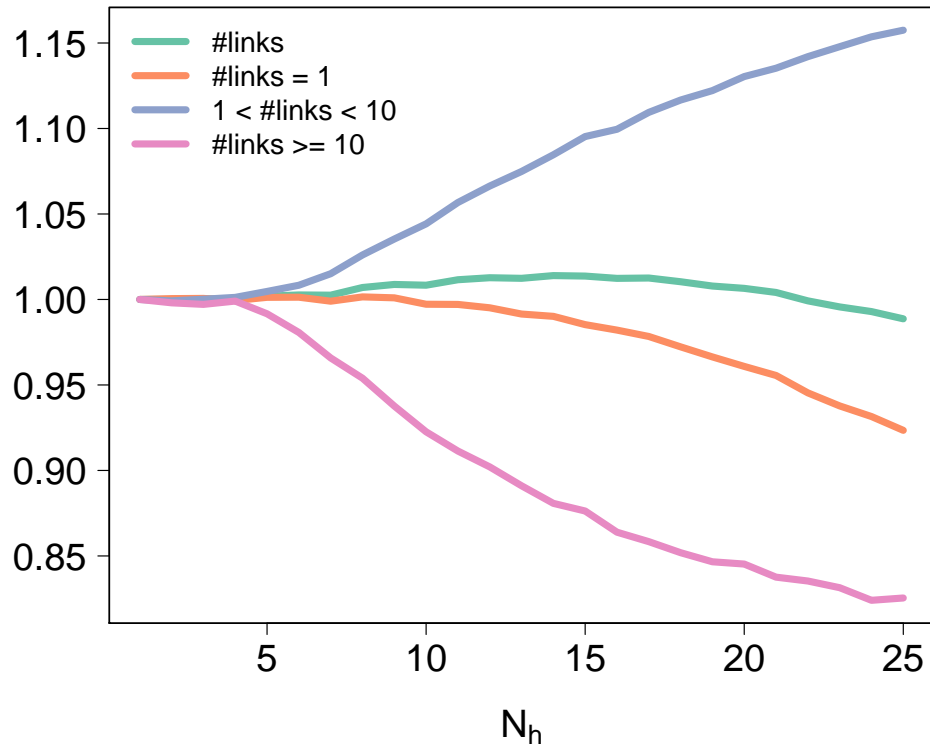


Figure S6. Influence of N_h on the number of links. The values have been normalized by the value obtained with $N_h = 1$.

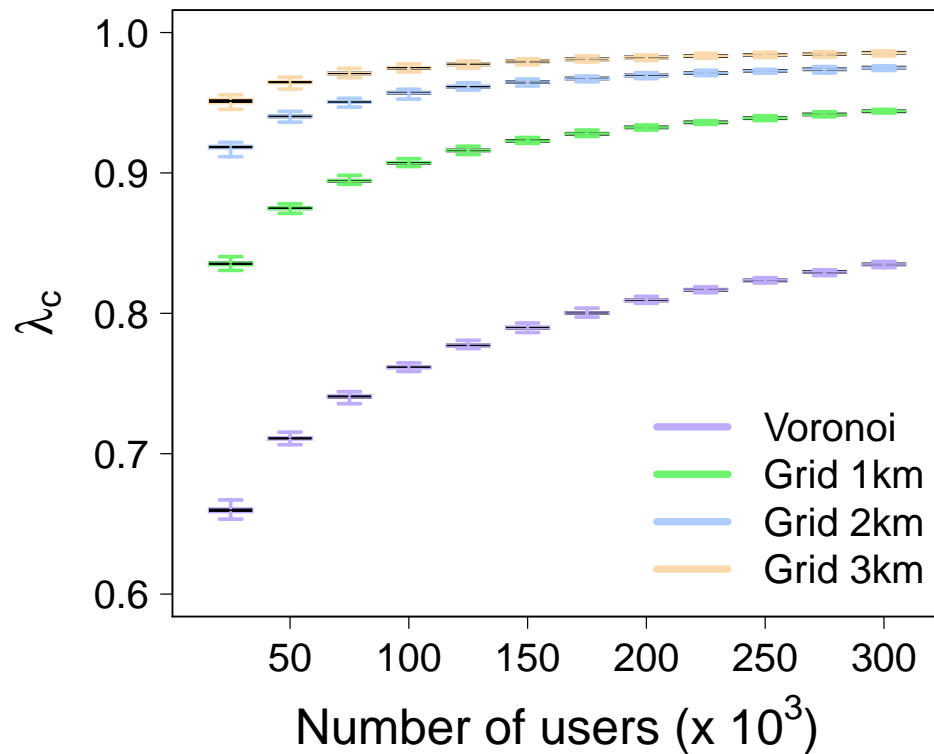


Figure S7. Influence of scale and sample size. Boxplots of λ_c as a function of the sample size according to the spatial scale (Voronoi cells and grid cells of 1, 2 and 3 km side length). The distributions are based on 100 independent comparisons with $N_d = 4$, $N_h = 12$ and $\delta_h = 1/3$. The whiskers correspond to the minimum and maximum of the distributions.

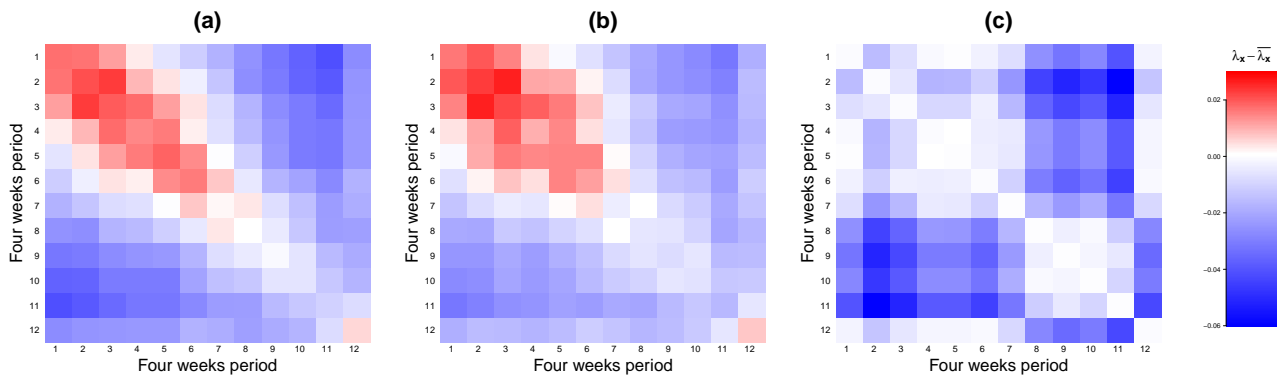


Figure S8. Temporal variations variations. Standard similarity metrics between ODs extracted at different time windows (four weeks periods, from the first week of January to the last week of November). (a) λ_c^* . (b) λ_l . (c) λ_d . The standardization has been obtained by subtracting average values obtained by comparing 100 independent samples based on 50,000 reliable users' home-work most visited locations drawn at random across the entire year. The values have been averaged over 100 independent comparisons based on 50,000 reliable users' home-work most visited locations at the Voronoi scale.